ELSEVIER

A separated flow model for predicting two-phase pressure drop and evaporative heat transfer for vertical annular flow

Feng Fu and James F. Klausner
University of Florida, Department of Mechanical Engineering, Gainesville, Florida, USA

A separated flow model has been developed that is applicable to vertical annular two-phase flow in the purely convective heat transfer regime. Conservation of mass, momentum, and energy are used to solve for the liquid film thickness, pressure drop, and heat transfer coefficient. Closure relationships are specified for the interfacial friction factor, liquid film eddy-viscosity, turbulent Prandtl number, and entrainment rate. Although separated flow models have been reported previously, their use has been limited, because they were tested over a limited range of flow and thermal conditions. The unique feature of this model is that it has been tested and calibrated against a vast array of two-phase pressure drop and heat transfer data, which include upflow, downflow, and microgravity flow conditions. The agreements between the measured and predicted pressure drops and heat transfer coefficients are, on average, better or comparable to the most reliable empirical correlations. This separated flow model is demonstrated to be a reliable and practical predictive tool for computing two-phase pressure drop and heat transfer rates. All of the datasets have been obtained from the open literature.

Keywords: two-phase annular flow; convective heat transfer; pressure gradient

Introduction

Two-phase annular flow patterns with heat transfer are prevalent in many industrial processes. The reliable prediction of pressure drop and heat transfer rates associated with these processes are essential to developing more reliable, efficient and cost effective heat exchangers; reducing or eliminating costly shutdowns caused by equipment failure; and achieving energy savings through optimization of thermal processes.

The annular flow pattern is one that frequently occurs in conjunction with evaporative heat transfer in tubes. Annular flow is characterized by an inherently unsteady liquid film flowing along the wall parallel to a flowing vapor core carrying entrained liquid droplets. The liquid film structure is influenced by many system variables, some of which are system geometry, flow orientation (up, down, microgravity, or horizontal flow), and liquid/vapor velocity difference. Kenning and Cooper (1989) identified two heat transfer regimes associated with evaporative two-phase flow heat transfer: the convective regime and the nucleate boiling regime. In the convective regime, nucleate boiling is completely suppressed, and the heat transfer is governed by bulk turbulent motion of the liquid film. Heat transfer in the nucleate boiling regime is governed by the incipience, growth, and departure of vapor bubbles along the heating surface. Klausner and Mei (1995) and Thorncroft et al. (1996) recently identified a dimensionless variable that can discriminate the convective and nucleate boiling heat transfer regimes. This work is specifically concerned with two-phase annular upflow, downflow, and microgravity flow pressure drop and evaporative heat transfer in the convective regime.

Analytical two-phase flow models typically treat the flow as steady, simplify the geometry of the flow structure, and use conservation of mass, momentum, and energy to predict pressure drop and heat transfer rates. Such models are attractive, because they attempt to physically model the dominant heat and momentum transport mechanisms, and thus there exists potential for such models to have broad applicability. They also give detailed information on the flow and thermal fields. The drawback of these models is that they require empirical closure relations, and typically these are tested against only a limited range of data. Two-dimensional (2-D) finite-difference models have been proposed by Lai (1992) for flow boiling and Mandrusiak and Carey (1990) for annular flow with offset strip fins. Separated flow models are those in which one-dimensional (1-D) conservation equations are applied separately to the vapor core and liquid film, and are coupled through closure relations applied at the liquid/vapor interface. Separated flow models have been discussed in detail by Hewitt and Hall-Taylor (1970), Carey (1992), and some more recent models have been proposed by Stevanovic and Studovic (1995), Owen and Hewitt (1987), and Sun et al. (1994). These models have only been calibrated over a narrow range of parameters and, thus, do not have broad applicability.

In this work a separated flow model, boundary conditions, and closure relations are presented as analytical tools to predict pressure drop and heat transfer rate for two-phase annular upflow, downflow, and microgravity flow in tubes. An extensive

Address reprint requests to Dr. J. F. Klausner, University of Florida, Department of Mechanical Engineering, P.O. Box 11630, Gainesville, FL 32611-6300, USA.

Received 28 August 1996; accepted 4 February 1997

Int. J. Heat and Fluid Flow 18: 541–549, 1997

655 Avenue of the Americas, New York, NY 10010

0142-727X/97/$17.00
PII S0142-727X(97)00001-5

experimental database has been compiled, and the empirical closure relations are calibrated against those data. It is demonstrated that separated flow modeling is a reliable alternative to empirical pressure drop and heat transfer correlations. This approach is a significant departure from the majority of two-phase heat transfer correlations, which attempt to cover both the convective and nucleate flow boiling regimes.

Separated flow model formulation

Consideration is given to the flow configuration depicted in Figure 1, in which there exits cocurrent annular flow with entrainment through a round tube and heat input at the wall. The following assumptions are inherent in the model: (1) the flow is incompressible; (2) the flow is steady; (3) the liquid film thickness is uniform around the tube periphery; (4) the liquid/vapor interface is smooth; (5) the pressure is uniform in the radial direction; (6) evaporation occurs at the liquid/vapor interface; and (7) liquid droplets entrained in the vapor core are uniformly distributed.

Conservation equations

Following Hewitt and Hall-Taylor (1970) a force balance on a cylidrical element of the liquid film in which acceleration is ignored leads to,

$$\tau = \tau_i\left(\frac{r_i}{r}\right) + \frac{1}{2}\left(\frac{dp}{dz} \pm \rho_l g\right)\left(\frac{r_i^2 - r^2}{r}\right) \tag{1}$$

and using the concept of eddy-viscosity,

$$\frac{du}{dy} = \frac{\tau}{\mu_l + \varepsilon_m \rho_l} \tag{2}$$

where τ is the shear stress, dp/dz is the axial pressure gradient, ρ is the density, g is the gravitational acceleration, u is the velocity, μ is the dynamic viscosity, ε_m is the eddy-viscosity, r is the radial coordinate, y is the distance from the wall, the subscripts i and l, respectively, denote the liquid/vapor interface and the liquid, and the + applies to upflow; whereas, − applies to downflow. Equations (1) and (2) may be combined, which results in

$$\frac{du}{dy} = \frac{\tau_i}{\mu_l + \varepsilon_m \rho_l}\left(\frac{r_0 - \delta}{r_0 - y}\right) + \frac{1}{2}\left(\frac{dp}{dz} \pm \rho_l g\right)\left(\frac{r_0 - y}{\mu_l + \varepsilon_m \rho_l}\right)\left[\left(\frac{r_0 - \delta}{r_0 - y}\right)^2 - 1\right] \tag{3}$$

where r_0 is the pipe radius, and δ is the liquid film thickness. Following Hewitt and Hall-Taylor (1970), a momentum balance

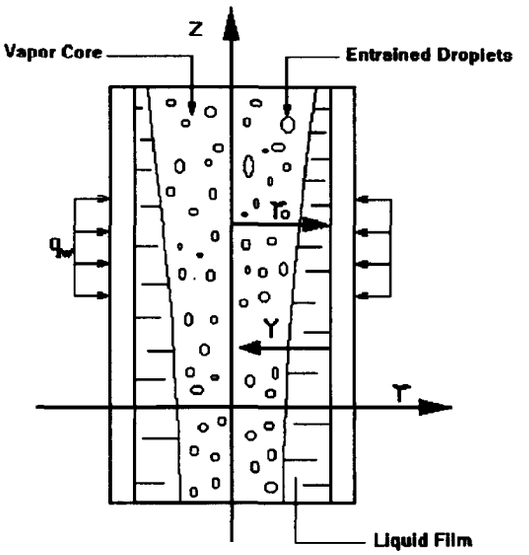

Figure 1 Idealized sketch of annular flow with heat transfer

Notation

B_o boiling number ($= q_w/Gh_{fg}$)
C_0 empirically determined distribution parameter
d_t pipe diameter, m
$\frac{dp}{dz}$ pressure gradient (Pa/m)
E entrainment rate
f friction factor
h heat transfer coefficient (W/m^{2}K)
h_{fg} latent heat of vaporization (J/kg)
g gravitational acceleration (m/s^2)
G total mass flux (kg/m^2 s)
Pr_t turbulent Prandtl number ($= \varepsilon_m/\varepsilon_H$)
q_w wall heat flux (W/m^2)
r radial coordinate, m
r_0 pipe radius, m
Re_l liquid phase Reynolds number ($= G(1-x)d_t/\mu_l$)
Re_v vapor-phase Reynolds number ($= Gxd_t/\mu_v$)
T temperature, °C
u velocity (m/s)
u^* friction velocity [$= \sqrt{(\tau_0/\rho)}$]
x quality
V_{vj} empirically determined drift velocity (m/s)
y radial coordinate, m
y^+ wall units ($= yu^*\rho/\mu$)
z axial coordinate, m

Greek

α void fraction
δ liquid film thickness, m
ε_m eddy-viscosity (m^2/s)
ε_H eddy thermal diffusivity (m^2/s)
η thermal diffusivity (m^2/s)
μ dynamic viscosity (kg/ms)
ρ density (kg/m^3)
σ interfacial tension (N/m)
τ shear stress (N/m^2)

Subscripts

i interfacial
l liquid
o wall
sat saturation
v vapor
2ϕ two-phase

on the vapor core, which includes momentum exchange due to entrainment, results in

$$\frac{dp}{dz} = -\left\{ \frac{2}{r_i}\tau_i \pm \frac{\rho_v g[x + E(1-x)]}{x + E(1-x)\frac{\rho_v}{\rho_l}} + \frac{G^2}{\alpha}\frac{d}{dz}\left[\frac{x^2}{\alpha\rho_v} + \frac{(1-E)^2(1-x)^2 x}{\rho_l(1-\alpha) - \rho_v \alpha E(1-x)} + \frac{E(1-x)x}{\alpha\rho_v} \right] \right\} \tag{4}$$

where E is the liquid mass fraction entrained in the vapor core, G is the total mass flux, x is the vapor quality, α is the vapor volume fraction, and the subscript v denotes the vapor. A mass balance on the liquid film is expressed as

$$\frac{r_0}{2}G(1-x)(1-E) = \rho_l \int_0^{\delta} u\left(1 - \frac{y}{r_0}\right) dy. \tag{5}$$

Consideration is now given to energy transport through the liquid film. Because turbulent diffusion across the thin film is typically much greater than convection downstream, a simplified energy equation is

$$\frac{d}{dy}\left[(\eta_l + \varepsilon_H)\frac{dT}{dy} \right] = 0 \tag{6}$$

where η_l is the liquid thermal diffusivity, and ε_H is the eddy thermal diffusivity. Assuming that the two-phase mixture is saturated, an energy balance dictates that the equilibrium vapor quality varies as

$$\frac{dx}{dz} = \frac{2q_w}{Gr_0 h_{fg}} \tag{7}$$

where q_w is the wall heat flux, and h_{fg} is the latent heat. The heat transfer coefficient is defined as

$$h_{2\phi} = \frac{q_w}{T_w - T_{sat}} \tag{8}$$

where T_w and T_{sat} are the respective wall and saturation temperatures. The required boundary conditions are

at the wall ($y = 0$):

$$u = 0, \quad q_w = -k_l \frac{dT}{dy}$$

and at the liquid/vapor interface ($y = \delta$):

$$\frac{du}{dy} = \frac{\tau_i}{\mu_l + \varepsilon_m \rho_l}, \quad T = T_{sat}.$$

Solution procedure

The relations above are not yet closed; they require that τ_i, ε_m, ε_H, and E be specified. The closure relations used for this model are discussed shortly. Given the appropriate closure relations, Figure 2 is a flowchart describing the solution procedure to the above equations, which is also summarized as,

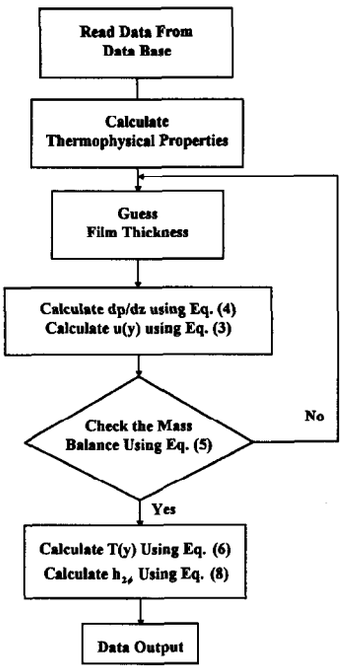

Figure 2 Flow chart of solution procedure

(1) An initial guess is made for the film thickness δ, and Equation 4 is used to compute the pressure gradient dp/dz.
(2) Equation 3 is used in conjunction with the velocity boundary conditions to compute the liquid film velocity profile $u(y)$.
(3) The velocity profile is used in Equation 5 to check if both sides of the equation balance.
(4) If both sides of Equation 5 balance, Equation 6 is used in conjunction with the temperature boundary conditions to compute the liquid film temperature profile $T(y)$, and the heat transfer coefficient defined in Equation 8 is evaluated. If Equation 5 does not balance, steps 1–3 are repeated.

Empirical closure relations

One of the most important variables that influences the solution of the separated flow model is the interfacial shear stress. After examining many different empirical correlations for interfacial shear stress, it has been found that a modified form of the correlation proposed by Henstock and Hanratty (1976) gives the best results. The equations required to compute the interfacial shear stress are as follows,

$$\tau_i = f_i \frac{1}{2}\rho_v u_v^2 \tag{9}$$

$$\frac{f_i}{f_s} = 1 + 1400F\left\{ 1 - \exp\left[-\frac{(1+1400F)^{1.5}}{13.2G_0 F} \right] \right\} \tag{10}$$

$$F = \frac{\left[(0.707\mathrm{Re}_{lf}^{0.5})^{2.5} + (0.0379\mathrm{Re}_{lf}^{0.9})^{2.5} \right]^{0.4}}{\mathrm{Re}_v^{m2}} \left(\frac{u_l}{\mu_v} \right)^{m1} \left(\frac{\rho_v}{\rho_l} \right)^{0.4} \tag{11}$$

where

$$u_v = \frac{Gx}{\rho_v}, \quad \mathrm{Re}_v = \frac{Gx2r_0}{\mu_v}, \quad \mathrm{Re}_{lf} = \frac{G(1-x)(1-E)2r_0}{\mu_l}$$

$$f_s = 0.046\mathrm{Re}_v^{-0.2}, \quad G_0 = \frac{2r_0 g\rho_l}{f_s \rho_v u_v^2}.$$

In Equation 11 m1 and m2 have been empirically determined based upon the available pressure drop data. For water m1 = 1.0, and m1 = 1.2 for all other fluids tested. It has also been found that m2 = 0.70 gives the best fit for the upflow data, while m2 = 0.80 gives the best fit for the downflow data.

Detailed turbulence measurements for annular flow liquid films are not available. The usual practice in treating the liquid film eddy-viscosity is to assume the wall turbulence is similar to that of single-phase flow and use single-phase flow correlations for the liquid film eddy-viscosity. Although such an assumption has yet to be experimentally validated, modified single-phase flow eddy-viscosity and turbulent Prandtl number correlations will be used here. Following the discussion of Kays (1994), the liquid film eddy-viscosity and turbulent Prandtl number are respectively computed from

$$\frac{\varepsilon_m}{\upsilon} = 0.001y^{+3} \qquad y^+ < 5$$

$$\varepsilon_m = \left\{Ky\left[1-\exp\left(-\frac{y^+}{25}\right)\right]\right\}^2 \left|\frac{du}{dy}\right| \left(1.0-\frac{y}{\delta}\right)^n \phi \qquad y^+ \geq 5 \quad (12)$$

and

$$\mathrm{Pr}_t = 1.07 \qquad y^+ < 5$$

$$\mathrm{Pr}_t = 1 + 0.855 - \tanh[0.2(y^+ - 7.5)] \qquad y^+ \geq 5 \quad (13)$$

where $K = 0.41$ is Von Karman's constant, $y^+ = yu^*/\upsilon$, $\mathrm{Pr}_t = \varepsilon_m/\varepsilon_H$, $u^* = (\tau_o/\rho_l)^{1/2}$, and τ_o is the shear stress at the wall. The damping factor $(1-y/\delta)^n$ appearing in Equation 12 is based on the suggestion of Levich (1962) that the turbulence is suppressed near the liquid/vapor interface. It has been found that $n = 1.5$ gives the best fit to the data. The factor ϕ has been introduced in Equation 12 to account for enhanced turbulence in the liquid film caused by the disturbance created by the evaporation radial momentum flux and is expressed as follows:

$$\phi = B_o^{0.3}\left(\frac{1-x}{x}\right)^{0.1} \quad (14)$$

where the boiling number is defined as $B_o = q_w/Gh_{fg}$. Evidence that the bulk turbulence is enhanced with evaporation is provided by Klausner et al. (1990), where it is shown that under otherwise identical flow conditions, the frictional pressure gradient increases with increasing heat flux.

It is noted that in implementing the solution procedure, an initial guess must be made for the friction velocity u^*. In subsequent iterations, u^* is computed from its definition and using Equation 2 to evaluate the wall shear stress.

Many correlations have been proposed for the liquid entrainment, but there tends to be a large scatter in the data, and most of these correlations have been based on air/water systems. Instead of using an entrainment correlation, it is noted that the mass fraction of liquid entrained in the vapor core is related to the liquid film thickness and vapor volume fraction through

$$E = \left[1 - \frac{\alpha}{(1-\delta/r_0)^2}\right]\frac{x}{1-x}\frac{\rho_l}{\rho_v} \quad (15)$$

and a Zuber–Findlay (1965) type model that has demonstrated success in predicting vapor volume fraction is instituted.

$$\alpha = \frac{1}{C_0\left(1+\frac{1-x}{x}\frac{\rho_v}{\rho_l}\right) + V_{vj}\frac{\rho_v}{Gx}} \quad (16)$$

where C_0 is an empirically determined distribution parameter, and V_{vj} is an empirically determined drift velocity. Klausner et al. (1990) have recommended that for upflow $C_0 = 0.98$ and $V_{vj} = 1.12$ m/s and for downflow $C_0 = 1.02$ and $V_{vj} = -0.11$ m/s. If values of C_0 and V_{vj} are known for a specific geometry, fluid,
and operating condition, those values should be used in Equation 16.

Database

An attempt has been made to put together a database that covers a wide range of flow and thermal conditions. Although various proprietary two-phase flow databases are in existence, this work is confined to the data reported in the open literature. Although this database is not exhaustive, it does cover a wide enough range of flow and thermal conditions to validate the proposed model. Table 1 describes the pressure drop database. Both adiabatic air/water mixtures and evaporating refrigerants are considered. The mass flux spans an order of magnitude, and the pipe diameter varies by more than a factor of 2. Vertical upflow, downflow, and microgravity flow data are considered. The air/water pressure drop data and microgravity data have

Table 1 Description of pressure drop database

Authors	Flow orientation	Fluid	Test section surface/diameter	Mass flux, kg/m²s	Quality	Heat flux, kW/m²	# of data points
Klausner (1989)	Up & down	R11	Copper/19.1	138 ~ 401	0.01 ~ 0.43	0.0 ~ 11	80
Shearer and Nedderman (1965)	Up	Water–air	Perspex/31.75 & 15.88 mm	40 ~ 186	0.73 ~ 0.99	*	24
Hall Taylor et al. (1963)	Up	Water–air	Perspex/31.75 mm	34 ~ 76	0.41 ~ 0.78	*	18
Hewitt et al. (1964)	Up	Water–air	Acrylic resin/31.75 mm	35 ~ 147	0.16 ~ 0.86	*	20
Andreussi et al. (1978)	Down	Water–air	Plexiglass/24 mm	68 ~ 375	0.12 ~ 0.72	*	45
Asali (1983)	Up	Water–air	Plexiglass/22.9 & 42 mm	25 ~ 256	0.19 ~ 0.97	*	99
Jallouk (1974)	Up	R114	Copper/19.9 mm	154 ~ 4677	0.01 ~ 0.84	4 ~ 50	563
Miller et al. (1993)	Micro-*g*	R12	Smooth tube/4.6 & 10.5 mm	83 ~ 571	0.10 ~ 0.94	*	110

* denotes adiabatic.

Table 2 Description of heat transfer database

Authors	Flow orientation	Fluid	Test section surface/diameter	T_{sat} °C	Mass flux, kg/m^{2}s	Quality	Heat flux, kW/m^2	# of data points
Bennet (1976)	Up	Water	Inconel/19.1 mm	121	184 ~ 1590	0.01 ~ 0.20	140 ~ 580	256
Klausner (1989)	Up & down	R11	Copper/19.8	32.4 ~ 51.4	130 ~ 400	0.001 ~ 0.40	4.0 ~ 12.0	170
Jallouk (1974)	Up	R114	Copper/19.9 mm	35.8 ~ 94.6	158 ~ 2386	0.021 ~ 0.83	6.3 ~ 82	442
Kenning and Cooper (1989)	Up	Water	Cupronickel/9.6 mm	142.4	123 ~ 304	0.010 ~ 0.41	50.0 ~ 350	12
Pujol (1968)	Up & down	R113	15.8 mm	54.2 ~ 85.4	351 ~ 1734	0.002 ~ 0.50	12.0 ~ 49.0	278
Somerville (1962)	Down	n-Butanol	11.86 mm	122 ~ 156	666 ~ 2148	0.000 ~ 0.32	88.0 ~ 208	209
Hahne et al. (1989)	Up & down	R12	Copper/20 mm	25.5 ~ 45.5	311 ~ 1017	0.001 ~ 0.17	1.3 ~ 77.0	96
Wang (1981)	Up	Water	Stainless steel/9.7 mm	109 ~ 148	50 ~ 233	0.025 ~ 0.56	75.0 ~ 477	114
Lavin (1963)	Up	R12&R22	Copper/18.6 mm	26.2 ~ 32.6	680 ~ 3030	0.173 ~ 0.89	2.4 ~ 28.0	41

been reported to correspond to the annular flow regime. The upflow and downflow refrigerant data have been filtered so that only data corresponding to the annular flow regime according to the flow regime map of Hewitt and Roberts (1969) are included in the database.

Table 2 describes the heat transfer database. The heat flux, mass flux, and vapor quality span an order of magnitude; whereas, the tube diameter is confined to a narrow range. Water, refrigerants, and n-butanol are considered. All of these datasets were filtered so that only data corresponding to the annular flow regime according to the map of Hewitt and Roberts (1969) are included. These datasets did not distinguish between the purely convective heat transfer regime and the nucleate boiling heat transfer regime. According to Klausner and Mei (1995) and

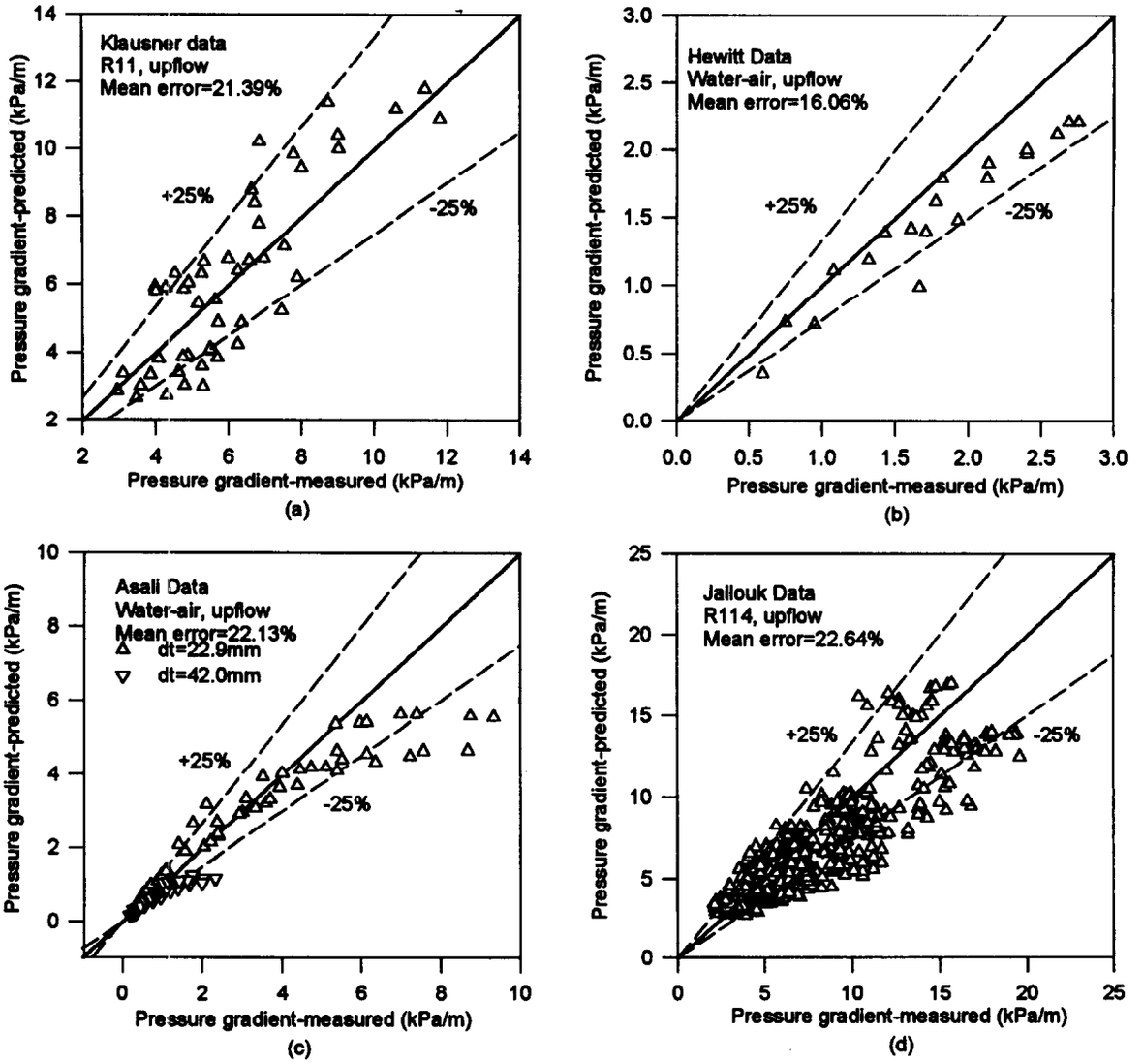

Figure 3 Comparison between measured and predicted pressure gradients for upflow

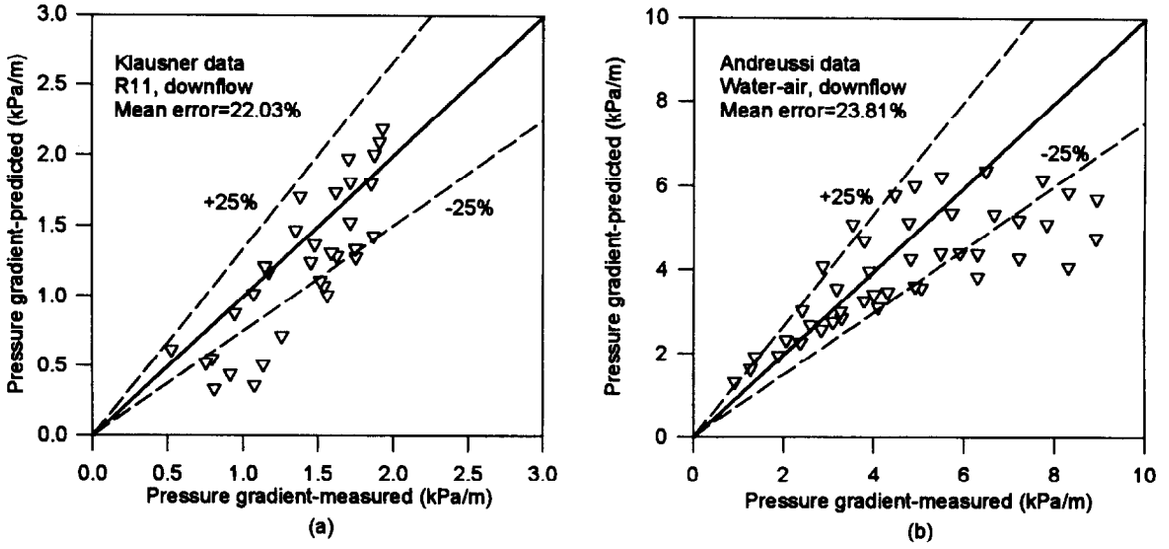

Figure 4 Comparison between measured and predicted pressure gradients for downflow

Thorncroft et al. (1996), the purely convective regime can be distinguished from the nucleate boiling regime using the dimensionless variable, r_{max}/r_{min}, which can be estimated as

$$\frac{r_{max}}{r_{min}} = \frac{\Delta T_{sat} k_l \rho_v h_{fg}}{h_{max} T_{sat} 2\sigma} \tag{17}$$

where h_{max} is the heat transfer coefficient caused by bulk turbulent convection, and σ is the interfacial tension. Here r_{max} and r_{min} are the respective maximum and minimum cavity radii required for incipience. Only those data for which $r_{max}/r_{min} < 120$ are included in the database.

Results and Discussion

Pressure drop

The first step in calibrating the model required comparing the measured and predicted pressure gradients and adjusting the empirical constants in the hydrodynamic closure relations based upon these results. After many iterations, the empirical constants required for the closure relations previously described were optimized. Figures 3a–d compare the predicted and measured pressure gradients for representative vertical upflow datasets, which include R11, R114, and air/water. It is readily seen that for the majority of data, the deviation between the measured and predicted pressure gradients are within $\pm 25\%$. Figures 4a–b compare the predicted and measured pressure gradients for vertical downflow. Again, the majority of data are within $\pm 25\%$ deviation.

Miller et al. (1993) have measured annular two-phase pressure gradients under microgravity conditions that were obtained during short duration parabolic trajectories flown with a NASA KC-135 aircraft. Under such conditions, there is uncertainty whether the flow steadied out during the micro-g window. Nevertheless, the present model was compared against their 10.5-mm tube diameter data. The values for m2, C_0, and V_{vj} were, respectively, taken to be m2 = 0.75, $C_0 = 1.0$, and $V_{vj} = 0.5$ m/s. As observed in Figure 5, the agreement is very good.

To compare the present model with other separated flow model predictions, the mean error is defined as

$$\text{M.E.} = \frac{1}{N} \sum \frac{|X_m - X_p|}{X_m} \tag{18}$$

where X_m and X_p are the respective measured and predicted variable under consideration and N is the number of datapoints. Table 3 compares the mean error for all of the datasets with the present model, the Henstock and Hanratty (1976) correlation, the Asali et al. (1985) correlation, and the Chisholm (1967) correlation. It is seen that for the air/water data, the mean error for the present model is comparable to that of the three correlations. However, for the refrigerant data, the present model agrees significantly better with the measured data.

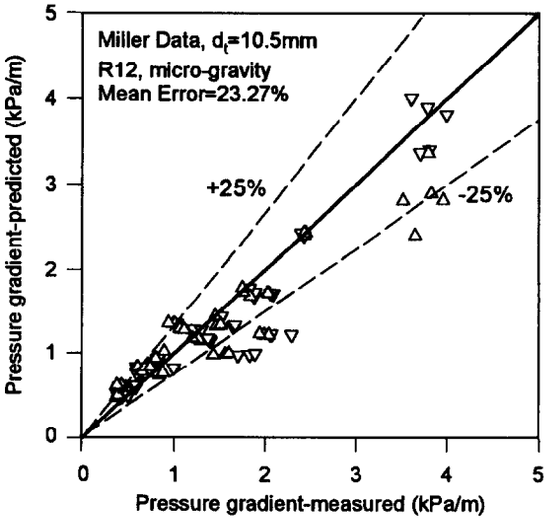

Figure 5 Comparison between measured and predicted pressure gradients for micro-gravity flow

Table 3 Comparison of pressure gradient mean error (%)

Data source	# of Datapoints	Present model	Henstock and Hanratty (1976)	Asali (1983)	Chisholm (1967)
Upflow:					
Klausner (1989)	60	19.68	32.29	40.62	25.55
Shearer et al. (1965)	24	15.97	19.58	15.30	12.76
Hall Taylor et al. (1963)	18	12.84	37.57	21.38	24.46
Hewitt et al. (1964)	20	16.06	16.57	20.16	24.25
Asali (1983)	99	22.13	25.77	18.33	14.76
Jallouk (1974)	563	22.64	45.51	40.40	50.74
Downflow:					
Klausner (1989)	20	27.56	42.84	49.31	33.43
Andreussi and Fanelli (1978)	45	23.81	45.27	17.32	6.25
Micro-*g*:					
Miller et al. (1993)	110	23.27	20.80	33.05	17.34

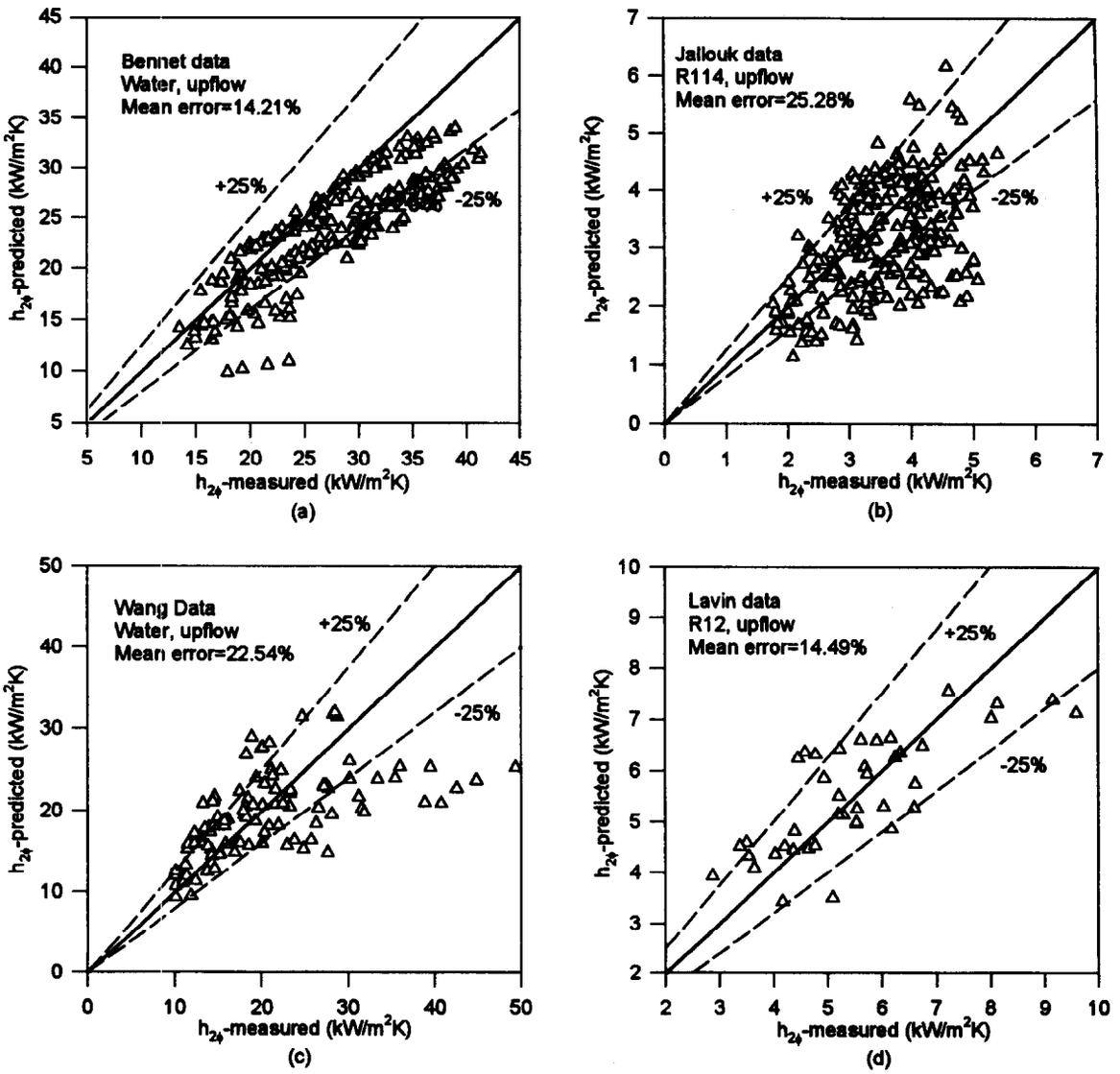

Figure 6 Comparison of measured and predicted heat transfer coefficients for upflow

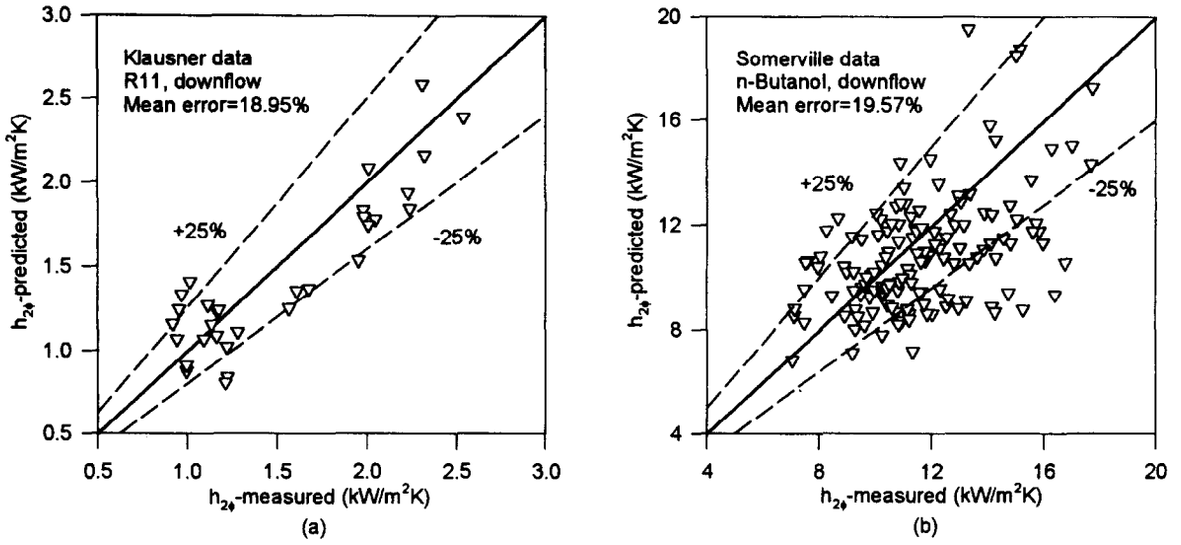

Figure 7 Comparison of measured and predicted heat transfer coefficients for downflow

Heat transfer

The final step in calibrating the model was to compare the measured and predicted heat transfer coefficients. It was found that the concept of turbulent Prandtl number was useful and the expression given by Kays (1994) for single-phase flow did not require any modification. Figures 6a–d compare the predicted and measured two-phase heat transfer coefficients for representative vertical upflow datasets, which include both refrigerants and water. It is seen that most of the data are within $+25\%$ deviation. For those data that deviate by more than $\pm 25\%$, the measured heat transfer coefficient is typically larger than that predicted. It is possible that some of these data fall into the nucleate boiling regime because there is some uncertainty in discriminating the purely convective regime from the nucleate boiling regime when $50 < r_{max}/r_{min} < 120$. Figures 7a–b compare the predicted and measured two-phase heat transfer coefficients for downflow. It is also seen that most of these data deviate by less than $\pm 25\%$. The mean error for all of the datasets are displayed in Table 4. When compared against the most recent flow boiling heat transfer correlations proposed by Gungor and Winterton (1986), Kandlikar (1989), and Steiner and Taborek (1992), it is seen that the present separated flow heat transfer model has slightly better agreement with most of the data identified to be in the purely convective heat transfer regime. The available micro-g heat transfer datasets do not provide sufficient information to allow a comparison with the present model.

The fact that this separated flow heat transfer model has such good agreement with a wide range of data lends credence to the contention of Klausner and Mei (1995) that many two-phase heat transfer data reported as flow boiling data are actually in the purely convective heat transfer regime.

Conclusions

The number of competing flow boiling heat transfer correlations that have been reported in the literature is vast. Many of those have been tested by Gungor and Winterton (1986), and none has proved to be satisfactory over the entire parameter space for which they were tested. Such correlations typically attempt to predict heat transfer rates in both the convective and nucleate flow boiling regimes.

In constrast, the present separated flow momentum and heat exchange model is applicable to upflow, downflow, and microgravity annular two-phase flow in the purely convective heat

Table 4 Comparison of heat transfer coefficient mean error (%)

Data source	# of Datapoints	Present model	Gungor and Winterton (1986)	Kandlikar (1989)	Steiner and Taborek (1992)
Upflow:					
Bennet (1976)	256	14.21	12.60	16.75	16.90
Klausner (1989)	105	15.47	17.14	14.78	18.88
Jallouk (1974)	442	25.28	28.95	32.09	37.58
Kenning and Cooper (1989)	12	25.11	49.07	36.90	38.66
Pujol (1968)	113	22.02	25.83	23.87	28.53
Hahne et al. (1989)	60	15.21	21.03	27.51	20.11
Wang (1981)	114	22.54	33.23	26.54	26.41
Lavin (1963)	41	14.49	16.86	22.71	15.42
Downflow:					
Klausner (1989)	65	17.80	15.05	14.88	18.96
Pujol (1968)	165	20.04	9.46	8.39	14.47
Somerville (1962)	209	19.57	19.06	28.43	16.06
Hahne et al. (1989)	36	19.90	22.52	25.06	20.32

transfer regime. Advantages of using the present model include the following.

(1) The same conservation equations are used to compute both the pressure gradient and heat transfer coefficient simultaneously.
(2) The predicted pressure gradient and heat transfer coefficient have been compared to and agree well with an extensive array of data that cover a wide range of flow and thermal conditions.
(3) As opposed to the majority of flow boiling heat transfer correlations, the model is based on fundamental conservation principles.
(4) The model provides information on the mean velocity and temperature fields in the liquid film.
(5) The equations used to solve for the pressure gradient and heat transfer coefficient are efficiently solved on a personal computer almost instantaneously.

We stress that because the model is closed with empirical relations, caution must be exercised when extending the model beyond the range of flow and thermal conditions for which it has been tested. Lastly, it has been demonstrated that separated flow modeling is a useful tool for predicting evaporative heat transfer in the purely convective regime.

Acknowledgments

This work was supported by the Exxon Education Foundation under grant No. 04/1995.

References

Andreussi, P. and Zanelli, S. 1978. Downward annular and annular-mist flow of air–water mixtures. *Proc. Intern. Seminar on Interface Transport in Liquid Films* (Dubrovrik, Yugoslavia)

Asali, J. C. 1983. Entrainment in vertical gas–liquid annular flow. Ph.D. thesis, University of Illinois at Urbana-Champaign, IL

Asali, J. C., Hanratty, T. J. and Andreussi, P. 1985. Interfacial drag and film height for vertical annular flow. *AIChE J.*, **31,** 895–902

Bennet, D. L. 1976. A study of internal forced convective boiling heat transfer for binary mixtures. Ph.D. thesis, Lehigh University, Bethlehem, PA

Carey, Van P. 1992. *Liquid–Vapor Phase–Change Phenomena*. Hemisphere, Bristol, PA

Chisholm, D. 1967. A Theoretical basis for the Lockhart–Martinelli correlation for two-phase flow. *Int. J. Heat Mass Transfer*, **10,** 1767–1778

Gungor, K. E. and Winterton, R. H. S. A. 1986. General correlation for flow boiling in tubes and annuli. *Int. J. Heat Mass Transfer*, **29,** 351–358

Hahne, E., Shen, N. and Spindler, K. 1989. Fully developed nuclear boiling in upflow and downflow. *Int. J. Heat Mass Transfer*, **32,** 1799–1808

Hall-Taylor, N., Hewitt, G. F. and Lacey, P. M. C. 1963. The motion and frequency of large disturbance waves in annular two-phase flow of air–water mixtures. *Chem. Eng. Sci.*, **18,** 537–552

Henstock, W. H. and Hanratty, T. J. 1976. The interfacial drag and the height of the wall layer in annular flows. *AIChE J.*, **22,** 990–1000

Hewitt, G. F. and Hall-Taylor, N. S. 1970. *Annular Two-Phase Flow*. Pergamon, New York

Hewitt, G. F., King, R. D. and Lovegrove, P. C. 1964. Liquid film and pressure drop studies. *Chem. Process Eng.*, 191–200

Hewitt, G. F. and Roberts, D. N. 1969. Studies of two-phase flow patterns by simultaneous x-ray and flash photography. *AERE-M 2159*, London

Jallouk, P. A. 1974. Two-phase flow pressure drop and heat transfer characteristics in vertical tubes. Ph.D. thesis, University of Tennessee at Knoxville, TN

Kays, W. M. 1994. Turbulent Prandtl number—Where are we? *J. Heat Transfer*, **116/285,** 284–295

Kandlikar, S. G. 1989. A general correlation for saturated two-phase flow boiling heat transfer inside horizontal and vertical tubes. *J. Heat Transfer*, **112,** 219–228

Kenning, D. B. R. and Cooper, M. G. 1989. Saturated flow boiling of water in vertical tubes. *Int. J. Heat Mass Transfer*, **32,** 445–458

Klausner, J. F. 1989. The influence of gravity on pressure drop and heat transfer in flow boiling. Ph.D. thesis, University of Illinois at Urbana-Champaign, IL

Klausner, J. F., Chao, B. T. and Soo, S. L. 1990. An improved method for simultaneous determination of frictional pressure drop and vapor volume fraction in vertical flow boiling. *Exper. Thermal Fluid Sci.*, **3,** 404–415

Klausner, J. F. and Mei, R. 1995. Suppression of nuclear sites in flow boiling. *Proc. Engineering Foundation Int. Conference on Convective Flow Boiling* (Paper no. IV-6)

Lai, J. C. H. 1992. Numerical simulation of two-dimensional steady-state and transient forced-convective boiling. Ph.D. thesis, Drexel University, Philadelphia, PA

Lavin, J. G. 1963. Heat transfer to refrigerants boiling inside plain tubes and tubes with internal turbulators. Ph.D. thesis, University of Michigan, Ann Arbor, MI

Levich, V. G. 1962. *Physicochemical Hydrodynamics*. Prentice-Hall, Englewood Cliffs, NJ, chapter XII

Mandrusiak, G. D. and Carey, V. P. 1990. A finite-difference computational model of annular film-flow boiling and two-phase flow in vertical channels with offset strip fins. *Int. J. Multiphase Flow*, **16,** 1071–1096

Miller, K. M., Ungar, E. K., Dzenitis and Wheeler, M. 1993. Microgravity two-phase pressure drop data in smooth tubing. In *Fluid Mechanics Phenomena in Micro-gravity*, AMD, Vol. 174, FED, Vol. 175, ASME, New York

Owen, D. G. and Hewitt, G. F. 1987. An improved annular two-phase flow model. *Proc. 3rd Int. Multiphase Flow Conference* (Paper no. C1), The Hague, The Netherlands

Pujol, L. 1968. Boiling heat transfer in vertical upflow and downflow in tubes. Ph.D. thesis, Lehigh University, Bethlehem, PA

Shearer, C. J. S. and Nedderman, R. M. 1965. Pressure gradient and liquid film thickness in co-current upwards flow of gas/liquid mixtures: Application to film-cooler design. *Chem. Eng. Sci.*, **20,** 671–683

Somerville, G. F. 1962. Downflow boiling of n-butanol in a uniformly heated tube. M.S. thesis, University of California, Lawrence Radiation Laboratory Rep. Livermore, CA, (UCRL-10527)

Steiner, D. and Taborek, J. 1992. Flow boiling heat transfer in vertical tubes correlated by an asymptotic model. *Heat Transfer Eng.*, **13,** 43–69

Stevanovic, V. and Studovic, M. 1995. A simple model for vertical annular and horizontal stratified two-phase flows with liquid entrainment and phase transitions: One-dimensional steady-state conditions. *Nuclear Eng. Design*, **154,** 357–379

Sun, G., Chan, W. H. G. T. and Hewitt, G. F. 1994. A general heat transfer model for two-phase annular flow. *Proc. Convective Flow Boiling Conference* (Paper no. IV-12)

Thorncroft, G. E., Klausner, J. F. and Mei, R. 1996. Suppression of flow boiling nucleation (to appear in Vol. 119 *J. Heat Transfer*, Aug. 1997)

Wang, S. W. 1981. A study of transition boiling phenomena with saturated water at 1–4 bar. Ph.D. thesis, University of Cincinnati, OH

Zuber-Findlay, 1965. Average volumetric concentration in two-phase flow systems. *J. Heat Transfer*, **87,** 453–468